

# Voltage Control Scheme in Distribution Network with Double Feed Induction Generator Wind Farm

JINGJING ZHAO<sup>a</sup>, XIN LI<sup>a</sup>, JUTAO HAO<sup>b</sup>

<sup>a</sup>State Key Laboratory of Power Transmission Equipment & System Security and New Technology  
Chongqing University  
400044 Chongqing  
CHINA

JingJingZhao@cqu.edu.cn

<sup>b</sup>School of Optical-Electrical and Computer Engineering  
University of Shanghai for Science and Technology  
200093 Shanghai  
CHINA

*Abstract:* - This paper presents the particle swarm optimization (PSO) for reactive power and voltage control (Volt/Var Control) in distribution system considering DFIG wind farm. In this paper, the reactive power output of DFIG wind farm has been considered as the control variables in the Volt/Var Control scheme by considering the reactive power compensation capability of DFIG. The minimization of total system real power loss and voltage deviation are utilized as an objective and the PSO is used to determine the reactive power output of DFIG wind farm, tap positions of load tap changer transformers (LTC) and numbers of the capacitor banks. Finally, the proposed scheme is applied to the 33-node distribution system. The results indicate that the proposed Volt/Var control scheme can improve the voltage profiles of distribution networks on a large scale.

*Key-Words:* - distribution network; DFIG wind turbine; wind farm; Volt/Var Control; particle swarm optimization

## 1 Introduction

In recent years, wind energy has grown to be one of the most important and promising sources of renewable energy [1-2]. Increasing wind power penetration has been noted to influence overall power system operation in terms of power quality, stability, voltage control, and security [3-5]. In weak power system, particularly in distribution network, since the X/R ratio of the distribution lines is small, the increased use of wind turbine for generating electricity makes voltage control more challenging, due to the unpredictable nature of wind conditions. Thus, the Volt/Var control in the distribution network with high level of wind power penetration becomes more of a concern, and it is necessary to examine how the Volt/Var control in the distribution network is affected by wind power.

Conventionally, Volt/Var control in distribution network can improve voltage profiles by adjusting load tap changer (LTC) of the substation transformer, voltage regulators and shunt capacitor or reactor banks [6-7]. Many researchers have investigated reactive power and voltage control in distribution networks. Reference [8] presented a heuristic and algorithmic combined approach for

reactive power optimization with time varying load demand in distribution systems. Reference[9] presented a genetic algorithm based procedure is used to determine both the load level partitioning and the dispatch scheduling. Reference[10] presented an improved evolutionary programming and its hybrid version combined with the nonlinear interior point technique to solve the optimal reactive power dispatch problems. Reference[11-12] presented methods for the Volt/Var control in radial distribution networks considering distributed generations.

However, the intermittent and stochastic characteristic of wind power generation may impact the stability and power quality issues of power systems, such as power fluctuations, voltage fluctuations, and harmonics [13]. The conventional Volt/Var control schemes can not solve these issues satisfactorily by the capacitor banks and LTC because the frequent switching of these devices may cause resonance and transient overvoltage, add additional stress on wind turbine gearbox and shaft, make themselves and turbines wear out quickly and increase the maintenance and replacement cost [14]. Therefore, additional compensating devices such as

static VAR compensator (SVC), static synchronous compensator (STATCOM) have been considered to address these issues more effectively because they provides the fast response time and superior voltage support capability [14-15]. However, there are always costs associated with the installation and operation of these devices, which makes this option less attractable, especially in the distribution network. Therefore, an alternative Volt/Var control scheme for DFIG wind farm becomes very important.

The variable-speed wind turbine equipped with doubly fed induction generator (DFIG) is the most employed generator for the recently built wind farm. The DFIG is able to obtain the maximum active power from wind speed and the generated reactive power can be controlled in an independent way without causing any interference in their active power generation process [16-18]. Utilizing DFIG reactive power control capability, wind farm composed of DFIG can be used as the continuous reactive power source to support system voltage control with fewer costs on the reactive power compensation device. This paper presents an innovative Volt/Var Control scheme in distribution system that does not require installation of additional compensating devices such as SVC and STATCOM to improve voltage regulation associated with the variable nature of the wind energy. The key to the Volt/Var Control scheme is to consider the reactive power output of DFIG wind farm as the control variables taking into account the reactive power compensation capability of DFIG.

Following this section, DFIG wind turbine model and the reactive power control capability are presented in Section 2. The formulation of the proposed problem is presented in Section 3. The basic mechanism of the particle swarm optimization and implementing the used PSO to Volt/Var control scheme is presented in Section4. In Section 5, the case of 33-node test system illustrates availability and correctness of the presented method. Finally, several important conclusions are given.

## 2 System model and control

### 2.1 Modeling of DFIG wind turbine

Fig.1 shows the model of DFIG wind turbine consisting of a pitch controlled wind turbine and an induction generator [19]. The stator of the DFIG is directly connected to the grid, while the rotor is connected to a converter consisting of two back-to-back PWM inverters, which allows direct control of the rotor currents. Direct control of the

rotor currents allows for variable speed operation and reactive power control thus DFIG can operate at a higher efficiency over a wide range of wind speeds and help provide voltage support for the grid. These characteristics make the DFIG ideal for use as a wind generator.

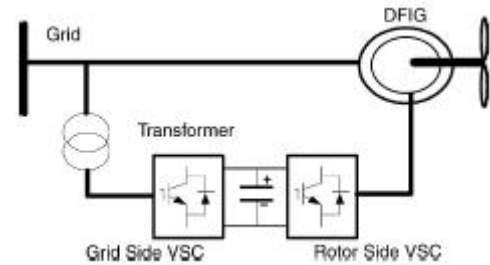


Fig.1 DFIG wind turbine

Fig. 2 shows the single-phase equivalent circuit of the DFIG in steady state [20]. The stator and rotor equations derived from this equivalent circuit are

$$\bar{U}_S = -R_S \bar{I}_S - jX_S \bar{I}_S - jX_M \bar{I}_R \quad (1)$$

$$\bar{U}_R = -R_R \bar{I}_R - jsX_R \bar{I}_R - jsX_M \bar{I}_S \quad (2)$$

where  $U_S$  is the stator voltage,  $U_R$  the rotor voltage,  $I_S$  the stator current,  $I_R$  the rotor current,  $R_S$  the stator resistance,  $R_R$  the rotor resistance,  $X_S$  the stator reactance,  $X_R$  the rotor reactance,  $X_M$  the mutual reactance, and  $s$  is the slip.

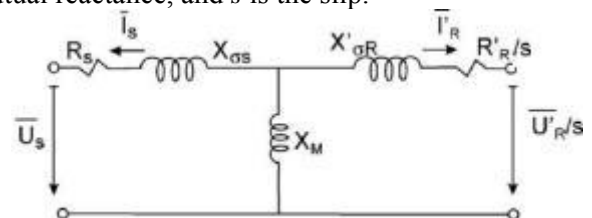


Fig.2. DFIG equivalent circuit

The total active power of the DFIG fed into the grid is the sum of stator and rotor active power [21].

$$P_T = P_S + P_R \quad (3)$$

Taking into account that

$$P_R = -sP_S \quad (4)$$

$$P_T = (1-s)P_S \quad (5)$$

where  $P_T$  is the total active power of the DFIG fed into the grid,  $P_S$  is the stator active power,  $P_R$  is the rotor active power.

Because rotor reactive power cannot flow through the frequency converter, so total reactive power fed into the grid is the sum of the stator and the grid side converter reactive power. Usually, in commercial systems, the grid side converter works with unity power factor, being total reactive power,

in such case, equal to stator reactive power.

$$Q_T = Q_S \tag{6}$$

The stator active and reactive power can be expressed as a function of stator current and rotor current [20]:

$$P_S^2 + Q_S^2 = (3U_S I_S)^2 \tag{7}$$

$$P_S^2 + (Q_S + 3\frac{U_S^2}{X_S})^2 = (3\frac{X_M}{X_S} U_S I_R)^2 \tag{8}$$

In the PQ plane, (7) represents a circumference centered at the origin with radius equal to the stator rated apparent power. Equation (8) represents a circumference centered at  $[-3U_S^2 / X_S, 0]$  and radius equal to  $3X_M U_S I_R / X_S$ .

Introducing (5) and (6) into (7) and (8):

$$(\frac{P_T}{1-s})^2 + Q_T^2 = (3U_S I_S)^2 \tag{9}$$

$$(\frac{P_T}{1-s})^2 + (Q_T + 3\frac{U_S^2}{X_S})^2 = (3\frac{X_M}{X_S} U_S I_R)^2 \tag{10}$$

According to (9) and (10), we can see the apparent power available at each DFIG is not constant, because the slip  $s$  changes as the wind speed varies. Therefore, given the stator voltage, the stator and rotor maximum allowable currents allowed by DFIG, the DFIG capability limits are obtained.

### 2.2 DFIG wind turbine power curve

Generally, the reference value of the active power that a DFIG should generate is established through optimum generation curves, which provide the active power as a function of the generator rotational speed. Such curves are derived as a result of analysis of the wind turbine aerodynamics, and by defining the maximum mechanical power the DFIG can extract from the wind at any angular speed [22-23]. Fig.3 shows the typical power curve for a 1500kW DFIG wind turbine.

### 2.3 DFIG wind turbine capability limits curve

Fig.4 shows the capability limits curves of 1500kW DFIG. The electric parameters of 1500kW DFIG are given in Table 1. In this figure, the solid and dashed curves correspond to equation (9) and equation (10) respectively, which represent the maximum reactive power that DFIG can generate or absorb at the rated stator voltage, maximum stator

current and rotor current. In Fig.4, The DFIG can be able to operate at any point in the intersecting area within the given limits. From Fig.4, one can observe that when the available active power  $P_T$  at the wind turbine is obtained, the reactive power output of the DFIG can be controlled to operate at any point in the intersecting area within the limit  $[Q_{T\min}, Q_{T\max}]$ .

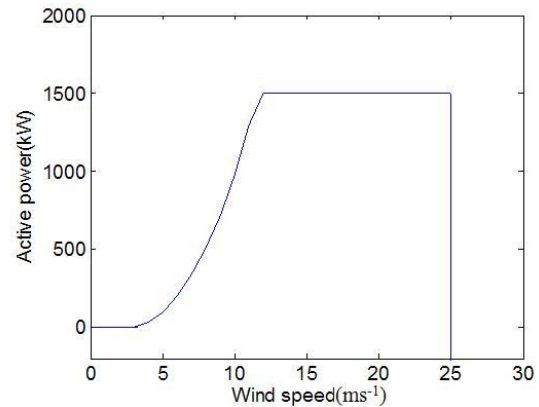


Fig.3 Power curve of a 1500kW DFIG wind turbine

Table 1 DFIG electric parameters

Parameter	Value
$R_S$ , stator resistance per phase	0.001692Ω
$X_S$ , stator leakage reactance per phase	0.03692Ω
$X_M$ , mutual reactance	1.4568Ω
$R_R$ , rotor resistance per phase	0.002423Ω
$X_R$ , rotor leakage reactance per phase	0.03759Ω

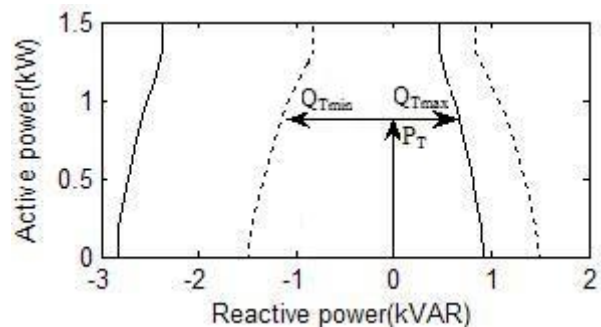


Fig.4. 1500kW DFIG capability limits curve

### 2.4 Wind farm model

In this paper, a wind farm model is developed with DFIG wind turbines connected in parallel. On a practical wind farm, each wind turbine has somewhat different instantaneous wind speed and output active power. Consequently, the capacity for reactive power generation of each wind turbine is also different. In this paper, we consider the total active and reactive power output of the wind farm

equal to the sum of the active and reactive power generated by each of the DFIG wind turbine in the wind farm:

$$P_{WF} = \sum_{i=1}^n P_{Ti} \quad (11)$$

$$Q_{WF} = \sum_{i=1}^n Q_{Ti} \quad (12)$$

where  $P_{WF}$  represents the active power output of the wind farm,  $Q_{WF}$  represents the reactive power output of the wind farm,  $P_{Ti}$  represents the generated active power of each  $i$  DFIG and  $Q_{Ti}$  represents the generated or absorbed reactive power of each  $i$  DFIG.

### 2.5 Load Flow including Wind Farm

In this paper, the node integrating DFIG based wind farm is treated as PQ nodes in a load flow analysis. In situations where the wind speed at wind farm is specified and the loads at buses are known, the real power output of DFIG can be calculated by means of the power curve. The reactive power of the wind farm is obtained from the optimization algorithm proposed in this paper. Then a backward-forward load flow algorithm is utilized to determine the real and reactive current injection at all the buses. Using these currents and a backward-forward sweep scheme the branch currents are found and voltages at all the buses are updated for this iteration.

## 3. Problem formulation

In this paper, the Volt/Var control in distribution networks considering wind farm is formulated as a mixed-integer nonlinear optimization problem by using the reactive power output of wind farm, reactive power of capacitors and tap positions of transformers as the control variable. The objective function and constraints are presented as follows:

### 3.1 Objective function

In this paper, the objective function is weighted summation of voltage deviations and electrical energy losses of distribution systems during the next day.

$$\min f_1(\bar{X}) = \lambda_1 \sum_{i=1}^{N_t} R_i \frac{P_i^2 + Q_i^2}{|V_i|^2} + \lambda_2 \max |V_i - V_{rat}| \quad (13)$$

$$\bar{X} = [\overline{Tap}, \overline{S_C}, \overline{Q_{WF}}]$$

$$\overline{Tap} = [Tap_1, Tap_2 \dots Tap_i \dots Tap_{N_t}]$$

$$\overline{S_C} = [Sc_1, Sc_2 \dots Sc_i \dots Sc_{N_c}]$$

where  $N_t$  is the total number of branches,  $V_i$  and  $V_{rat}$  are the real and rated voltage on bus  $i$ .  $\lambda_1$  and  $\lambda_2$  represent weighting factors.  $\lambda_1 + \lambda_2 = 1$ .  $\bar{X}$  denotes state variables vector,  $\overline{Q_{WF}}$  is the wind farm reactive power vector,  $\overline{Tap}$  is tap vector representing tap position of all transformers,  $\overline{Tap}_i$  is tap position of the  $i$ th transformer,  $\overline{S_C}$  is capacitors switching state vector including state of all capacitors,  $\overline{S_C}_i$  is the number of the  $i$ th capacitor bank.  $N_c$  is the number of capacitors,  $N_t$  is the number of transformers.

### 3.2 Constraints

The minimization of the objective function is subjected to the following constraints:

1) Distribution power flow equations:

$$P_i + P_{WFi} = P_{Di} + V_i \sum_{j=1}^{Nb} V_j (G_{ij} \cos \delta_{ij} + B_{ij} \sin \theta_{ij}) \quad (14)$$

$$Q_i + Q_{WFi} = Q_{Di} + V_i \sum_{j=1}^{Nb} V_j (G_{ij} \sin \delta_{ij} - B_{ij} \cos \theta_{ij}) \quad (15)$$

Where  $P_i$  and  $Q_i$  are the substation injected active and reactive power at the  $i$ th bus.  $P_{WFi}$  and  $Q_{WFi}$  are the wind farm injected active and reactive power at the  $i$ th bus.  $P_{Di}$ ,  $Q_{Di}$  are the active and reactive load power at the  $i$ th bus.  $V_i$  and  $V_j$  are the amplitude of voltage at the  $i$ th and  $j$ th bus, respectively.  $G_{ij}$  and  $B_{ij}$  are the conductance and the susceptance between the  $i$ th and  $j$ th nodes.  $\delta_{ij}$  and  $\theta_{ij}$  are the phase angle difference between the  $i$ th and  $j$ th nodes.

2) DFIG wind turbine active capacity limits:

$$P_{Ti, \min} \leq P_{Ti} \leq P_{Ti, \max} \quad (16)$$

where  $P_{Ti}$ ,  $P_{Ti, \min}$  and  $P_{Ti, \max}$  are scheduled, minimum and maximum active power output of the  $i$ th DFIG, respectively.

3) DFIG reactive capacity limits:

$$Q_{Ti} \geq -\sqrt{\left(3 \frac{X_M}{X_S} U_S I_R\right)^2 - \left(\frac{P_{Ti}}{1-s}\right)^2} - 3 \frac{U_S^2}{X_S} \quad (17)$$

$$Q_{Ti} \leq \sqrt{\left(3 \frac{X_M}{X_S} U_S I_R\right)^2 - \left(\frac{P_{Ti}}{1-s}\right)^2} - 3 \frac{U_S^2}{X_S}$$

where  $Q_{Ti}$  is reactive power output of the  $i$ th DFIG wind turbine.

4) Tap of transformers:

$$Tap_{i,\min} < Tap_i < Tap_{i,\max} \quad (18)$$

where  $Tap_{i,\min}$ ,  $Tap_i$ ,  $Tap_{i,\max}$  are the minimum, maximum and current tap positions of the  $i$ th transformer, respectively.

5) Node voltage magnitude limits:

$$V_{\min} \leq V_i \leq V_{\max} \quad (19)$$

where  $V_i$  is the voltage magnitude of node  $i$ ,  $V_{\min}$  and  $V_{\max}$  are low and upper bound of nodal voltage, respectively.

6) Distribution line limits:

$$|P_{ij}^{line}| < P_{ij,\max}^{line} \quad (20)$$

where  $|P_{ij}^{line}|$  and  $P_{ij,\max}^{line}$  are absolute power flowing over distribution lines and maximum transmission power between nodes  $i$  and  $j$ , respectively.

7) Radial structure of the network.

### 3.3 Handling Constraints

When adopting PSO to solve the mixed-integer nonlinear optimization problem, the constraints are considered into the objective function using penalty terms. The control variables, including reactive powers output of wind farm, tap positions of transformers and numbers of the capacitor banks. are self-constrained when encoding them as particles. However, the state variables, including voltages of PQ buses and wind farm connecting buses are constrained as penalty terms into the integrative objective function as follows:

$$F(x) = f(x) + k_1 \sum_{j=1}^{Nu} U_j(x) + k_2 \sum_{j=i}^{Ne} E_j(x) \quad (21)$$

where  $f(x)$  is the objective function values of optimization problem.  $N_u$  and  $N_e$  are the number of inequality and equality constraints, respectively.  $U_j(x)$  and  $E_j(x)$  are the inequality and equality constraints.  $k_1$  and  $k_2$  are the penalty factors, respectively.

## 4 Volt/Var control problem using PSO

### 4.1 The Standard PSO

The PSO is a population-based optimization method first proposed by Kennedy and Eberhart [24]. The PSO algorithm is initialized with the

population of individuals being randomly placed in the search space and search for an optimal solution by updating individual generations. At each iteration, the velocity and the position of each particle are updated according to its previous best position ( $Pbest_i$ ) and the best position found by informants ( $Gbest$ ). Each particle's velocity and position are adjusted by the following formula:

$$v_i^k(t) = \omega \cdot v_i^k(t) + c_1 \cdot r_1 (Pbest_i^k(t-1) - x_i^k(t-1)) + c_2 \cdot r_2 (Gbest^k(t-1) - x_i^k(t-1)) \quad (22)$$

$$x_i^k(t) = x_i^k(t-1) + v_i^k(t) \quad (23)$$

where  $i$  is the number of the particle in the swarm,  $k$  is the number of element in the particle  $x_i(t)$ , and  $t$  is the iteration number.  $v_i^k(t)$  and  $x_i^k(t)$  are the velocity and the position of  $k$ th element of the  $i$ th particle at the  $t$ th iteration, respectively.  $r_1$  and  $r_2$  are the random numbers uniformly distributed between 0 and 1. The constants  $c_1$  and  $c_2$  are the weighting factors of the stochastic acceleration terms and  $\omega$  is the positive inertia weight.

The suitable selection of inertia weight  $\omega$  in (24) provides a balance between global and local explorations [25]. The inertia weight  $\omega$  can be dynamically set with the following equation:

$$\omega^{(t+1)} = \omega^{\max} - \frac{\omega^{\max} - \omega^{\min}}{t_{\max}} \times t \quad (24)$$

where  $t_{\max}$  is the maximum number of iteration, and  $t$  is the current iteration number.  $\omega^{\max}$  and  $\omega^{\min}$  are the upper and lower limits of the inertia weight.

### 4.2 Discrete PSO

The original PSO initially developed for problems defined over real-valued vector spaces can also be applied to discrete-valued search spaces where either binary or integer variables have to be arranged into particles.

1) BPSO

The BPSO algorithm was introduced by Kennedy and Eberhart to allow the PSO algorithm to operate in binary problem spaces [26]. It uses the concept of velocity as a probability that a bit takes on one or zero. In the BPSO, (22) for updating the velocity remains unchanged, but (23) for updating the position is re-defined by the rule:

$$\begin{cases} x_i^k(t) = 1, & r < S(v_i^k(t-1)) \\ x_i^k(t) = 0, & r \geq S(v_i^k(t-1)) \end{cases} \quad (25)$$

where  $S(v_i^k)$  is the sigmoid function for transforming the velocity to the probability as the following expression:

$$S(x) = \frac{1}{1 + e^{-x}} \quad (26)$$

## 2) Integer PSO

In a more general case, when integer solutions (not necessarily 0 or 1) are needed, the optimal solution can be determined by rounding off the real optimum values to the nearest integer. Equations (22) and (23), developed for a real number space, are used to determine the new position for each particle. Once  $x_i(t)$  is determined, its value in the  $k$ th dimension is rounded to the nearest integer value using the bracket function (27)

$$x_i^k(t) = [x_i^k(t)] \quad (27)$$

## 4.3 Volt/Var control problem using PSO

In this paper, Volt/Var control is formulated as a mixed-integer nonlinear optimization problem with continuous variables such as the reactive power output of wind farm and discrete variables such as the tap positions of transformers and numbers of the capacitor banks. In this paper, the expanded PSO is applicable to solve Volt/Var Control problem with continuous and discrete variables. The PSO can handle the whole mixed-integer nonlinear optimization problem easily and naturally.

The steps followed for the proposed VVC algorithm using the PSO are described as follows:

- Step 1: Input system data, wind speed and wind farm parameters. The initial population and velocity for each particle should be generated randomly within the constrain limits.
- Step 2: The objective function (21) is calculated for each individual by using the result of distribution load flow.
- Step 3: The individual that has the minimum objective function should be selected as the global position.
- Step 4: The  $i$ th individual is selected.
- Step 5: The best local position is selected for the  $i$ th individual.
- Step 6: The velocity and position of the  $i$ th individual should be updated according to equations (22) and (23).
- Step 7: After  $x_i(t)$  is determined, discrete

variables value such as the tap positions of transformers and numbers of the capacitor banks in the  $k$ th dimension is rounded to the nearest integer value using the equations (27).

Step 8: If all individuals are selected, go to the next step, otherwise  $i = i + 1$  and go to Step 2.

Step 9: If the maximum number of iteration is reached, the search procedure is stopped, otherwise go to Step 2.

## 5 Simulation results

In this part, the proposed Volt/Var Control considering wind farm has been applied to the 33-node distribution system given in Ref.[27] (see Fig.5). Voltage limits are assumed to be within the range 0.95–1.05p.u. To simplify analysis, we assume that loads are the constant in all time periods. A small wind farm comprising 4 DFIG wind turbines of 1500kW is connected at node 33 through a rated 12.66/0.69kV transformer. The performance parameters of 1500kW DFIG are given in Table 2. The LTC has 11 tap positions ( $1.00 \pm 5 \times 1\%$ ). Four shunt capacitor banks are installed in node 10, 14, 17, 31, respectively, the capacitor banks size are  $4 \times 300$ kVAR.

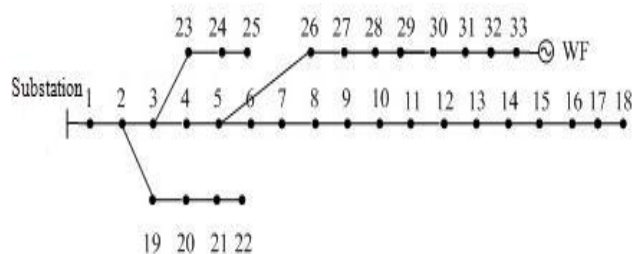


Fig.5 33-node distribution system

Table 2 1500kW DFIG Performance parameters

Parameter	Value
Rated capacity	1500 (kW)
Cut-in wind speed	4 (m/s)
Cut-out wind speed	25 (m/s)
Rated wind speed	12 (m/s)
Rated voltage	0.69 (kV)

The number of particles is set to 20 and the maximum iteration number of the algorithm is set to 100. The values of the parameters required for the implementation of the algorithm are  $c_1 = c_2 = 2.0$ ,  $\omega^{\max} = 0.9$  and  $\omega^{\min} = 0.4$ .

In this paper, different wind speeds were assumed

for the each wind turbine in the wind farm, the daily wind speed variation are changed as shown in Fig.6. The wind speed at each generator is considered to be constant during every period, one of which lasts one hour.

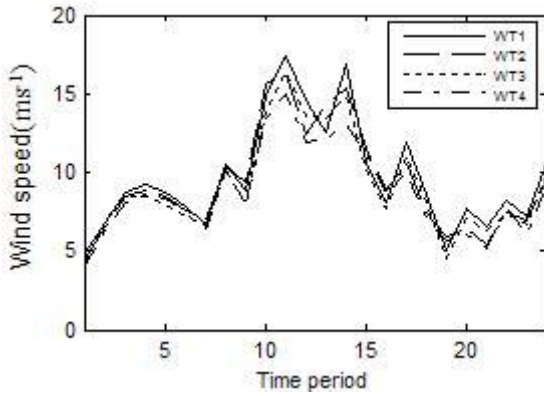


Fig.6 Curve of wind speed

The actual active power outputs of each DFIG in each period are shown in Fig.7, calculated by means of the power curve of each DFIG.

Choose five periods to analyze, the reactive power outputs limits of each DFIG in each period can be calculated according to equation (9) and (10), respectively, and the results are list in Table 3. It can be observed from Table 3 that wind farm made up of DFIG wind turbine can generate high quantities of reactive power when the available active power is far from its maximum. Taking period 1 as an

example, the average wind speed at wind farm is 4.9m/s, the maximum active power wind farm can generate are 0.3563MW, and the reactive power outputs limits of wind farm is from -4.2621MVAR to 3.6657MVAR. But the maximum reactive power wind farm can generate become very low when the available active power is near to its rated power. For example, in the period 5, the average wind speed is 14m/s, the active power that wind farm generated is rated power 5.9813MW, the reactive power outputs limits of wind farm is from -2.3970MVAR to 1.8220MVAR.

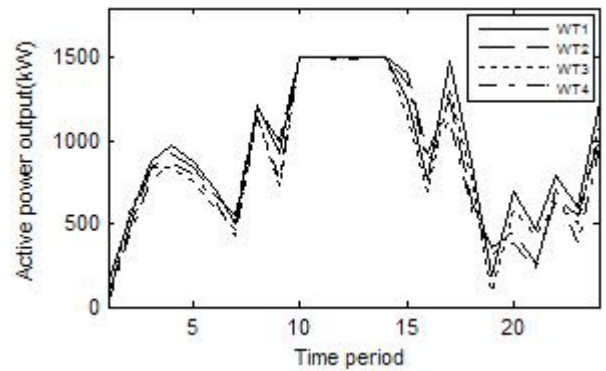


Fig.7 Active power of each DFIG wind turbine

According to the proposed Volt/Var Control scheme in this paper, the Volt/Var Control results of five periods are shown in Table 4.

Table 3 Wind speed and available power in wind farm

Period	Wind speed (m/s)	$P_{WF,max}$ (MW)	$Q_{WF,min}$ (MVAR)	$Q_{WF,max}$ (MVAR)
1	4.9	0.3563	-4.2621	3.6657
2	6.8	1.9875	-3.8562	3.2097
3	8.7	3.3375	-3.3216	2.7253
4	10.5	4.7064	-2.4135	1.9912
5	14.6	5.9813	-2.3970	1.8220

Table 4 Results of Volt/Var Control

Period	Tap position	C1	C2	C3	C3	$Q_{WF}$ (MVAR)	Loss (MW)
1	5	2	1	1	2	0.6816	0.2445
2	1	1	1	1	3	0.4530	0.1887
3	-2	2	2	1	2	-0.1598	0.4799
4	-3	2	3	1	4	-1.5686	1.0584
5	-2	2	2	2	3	-2.1212	1.9302

To demonstrate the performance of the proposed Volt/Var Control scheme, we compare the proposed Volt/Var Control to the conventional Volt/Var Control, which the power factor of wind farm keeps constant 0.98. Fig.8 (a)~(e) show the system voltage profiles for five periods after two different Volt/Var Control. In Fig.8, the line marked with hollow cylindrical represents the nodal voltage magnitudes after conventional Volt/Var Control, and the line marked filled circle represent the nodal voltage magnitudes after the proposed Volt/Var Control.

From Fig.8 it can be seen that, when the wind turbines operating at low wind speed, the active power output of the wind farm is small, the nodal voltage magnitudes after the proposed Volt/Var Control and the conventional Volt/Var Control all can maintain within the voltage allowable range as shown in Fig.8(a)~(c). But with increase in the wind speed and the real power output of the wind farm, the nodal voltage magnitudes near the point of common coupling can not maintain within voltage allowable range after the conventional Volt/Var Control, but utilizing the proposed Volt/Var Control in this paper, the nodal voltage magnitudes all maintain within the voltage allowable range as shown in Fig.8 (d)~(e). It can be concluded that the proposed Volt/Var Control scheme can improve voltage profile in the distribution system effectively associated with the variable nature of the wind energy without requiring installation of additional compensating devices such as SVC and STATCOM.

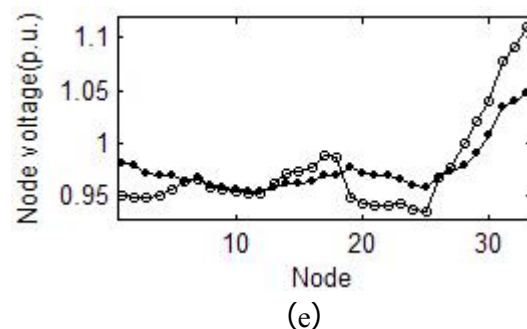
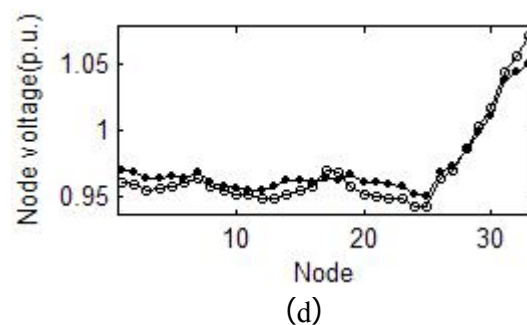
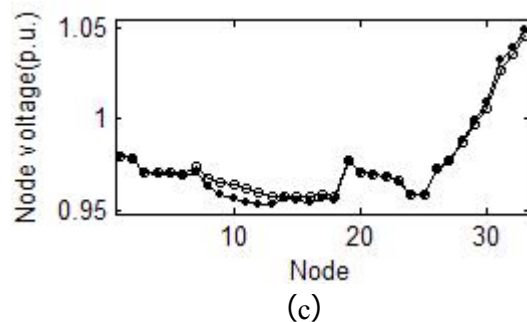
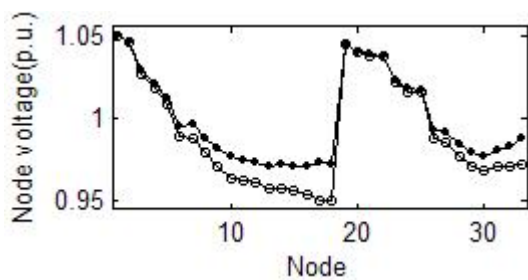
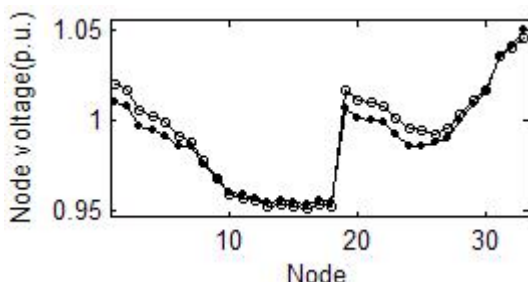


Fig.8 Nodal voltage distributions



(a)



(b)

## 6. Conclusions

In this paper, an innovative Volt/Var Control scheme in distribution system utilizing DFIG wind farm as reactive power compensation source is proposed. In the proposed Volt/Var Control scheme, reactive power output of wind farm is utilized as the control variable by taken into account DFIG reactive capability limits. From the results obtained in the simulations, it can be concluded that the proposed Volt/Var Control scheme can improve voltage regulation associated with the variable nature of the wind energy without requiring installation of additional compensating devices such as SVC and STATCOM.

### References:

- [1] M. Jefferson, Sustainable Energy Development: Performance and Prospects, *Renew Energy*, Vol.31, 2006, pp. 571–582.
- [2] G. Sideratos and N. D. Hatziargyriou, An Advanced Statistical Method for Wind Power

- Forecasting, *IEEE Trans. Power Syst.*, Vol. 22, No. 1, 2007, pp. 258–265.
- [3] J. Smajo, M. Smajo, D. Vukadinovic, Impact of Reference Value of Wind Turbine Active Power to the Distribution of Doubly-Fed Induction Generator Power, *WSEAS Transactions on Systems*, Vol. 5, No. 1, 2006, pp. 240-247.
- [4] K.S. Sandhu, S. Vadhera, Reactive Power Requirements of Grid Connected Induction Generator in a Weak Grid, *WSEAS Transactions On Circuits and Systems*, Vol. 7, No. 3, 2008, pp. 150-159.
- [5] J.J. Zhao, X. Li, C.L. Zhang, J.P. Lu. Joint Optimization Algorithm for Network Reconfiguration and Reactive Power Control of Wind Farm in Distribution System, *WSEAS Transactions on Circuit and Systems*, Vol.8, No. 2, 2009, pp. 268–279.
- [6] M. Baron, M. Hsu, Volt/Var Control at Distribution Substations, *IEEE Trans Power Syst*, Vol. 14, No. 1, 1999, pp. 312–318.
- [7] I. Roytelman, B. Wee, R. Lugtu, Volt/Var Control Algorithm for Modern Distribution Management System, *IEEE Trans Power Syst*, Vol. 10, No. 3, 1995, pp. 1454–1460.
- [8] Y. Deng, X. Ren, C. Zhao, D. Zhao, A Heuristic and Algorithmic Combined Approach for Reactive Power Optimization with Time Varying Load Demand in Distribution Systems, *IEEE Trans Power Syst*, Vol. 17, No. 4, 2002, pp. 1068–1072.
- [9] Z. Hu, X. Wang, H. Chen, G. Taylor, Volt/Var Control in Distribution Systems Using A Time-Interval Based Approach, *IEE Proc Gener Transm Distrib*, 2003, pp.548–554.
- [10] W. Lu, D. Yu, A Novel Optimal Reactive Power Dispatch Method Based on an Improved Hybrid Evolutionary Programming Technique, *IEEE Trans Power Syst*, Vol. 19, No. 2, 2003, pp. 913–918.
- [11] T. Niknam, A. Ranjbar, A. Shirani, Impact Of Distributed Generation on Volt/Var Control in Distribution Networks, *IEEE Bologna Power Tech Conference Proceedings*, 2003, pp. 1–6.
- [12] T. Niknam, A New Approach Based on Ant Algorithm for Daily Volt/Var Control in Distribution Networks Considering Distributed Generators, *Energy Conversion and Management*, Vol. 49, 2008, pp. 3417-3424.
- [13] A. Kehrlı and M. Ross, Understanding Grid Integration Issues at Wind Farms and Solutions Using Voltage Source Converter Facts Technology, *IEEE Pes Gen. Meeting*, Jul, 2003, pp. 1822–1827.
- [14] H. Chong, Q. H. Alex, M. E. Baran, et.al, Statcom Impact Study on the Integration of a Large Wind Farm into a Weak Loop Power System, *IEEE Trans Energy Conversion*, Vol. 23, No. 1, 2008, pp.226-234.
- [15] A. Papantoniou and A. Coonick, Simulation of Facts for Wind Farm Applications. *IEE Colloquium on Power Electronics for Renewable Energy*, June 1997, pp.1-5.
- [16] P. Cartwright, L. Holdsworth, J. B. Ekanayake, and N. Jenkins, Coordinated Voltage Control Strategy for a Doubly-Fed Induction Generator (DFIG)-Based Wind Farm, *IEE Proc. Generat. Transmiss. Distrib.*, Jul. 2004, pp.495–502.
- [17] D. J. Atkinson, R. A. Lakin, And R. Jones, A Vector-Controlled Doubly-Fed Induction Generator for a Variable-Speed Wind Turbine Application, *Transactions Of The Institute Of Measurement & Control*, Vol.19, No.1, 1997, pp.2–12.
- [18] R. S. Peña, J. C. Clare, And G. M. Asher, Vector Control of a Variable Speed Doubly-Fed Induction Machine for Wind Generation Systems, *Epe Journal*, Vol.6, No.3, 1996, pp.60–67.
- [19] L.M. Fernández, C.A. García, J.R. Saenz, et, al., Aggregated Dynamic Model for Wind Farms with Doubly Fed Induction Generator Wind Turbines, *Renewable Energy*, Vol.33, No.1, 2008, pp.129-140.
- [20] D. Santos-Martin, S. Arnaltes, J.L.R. Amenedo, Reactive Power Capability of Doubly Fed Asynchronous Generators, *Electric Power Systems Research*, Vol.78, No.11, 2008, pp.1837–1840.
- [21] L. Jiao, B. Ooi, G. Joós, F. Zhou, Doubly-Fed Induction Generator (DFIG) as a Hybrid of Asynchronous and Synchronous Machines, *Electric Power Systems Research*, Vol.76, No.3, 2005, pp. 33-37.
- [22] G. Tapia, A. Tapia, J.X. Ostolaza, Two Alternative Modeling Approaches for the Evaluation of Wind Farm Active and Reactive Power Performances, *IEEE Trans. On Energy Convers.*, Vol. 21, No. 4, 2006, pp. 909-920.
- [23] G. Tapia, A. Tapia, J. X. Ostolaza, Proportional Integral Regulator Based Approach to Wind Farm Reactive Power Management for Secondary Voltage Control, *IEEE Trans. on Energy Convers.*, Vol. 22, No. 2, 2007, pp. 448–459.
- [24] J. Kennedy, R. Eberhar, Particle Swarm Optimization. *IEEE International Conference on Neural Networks*, Perth, Australia, 1995.

- [25] Y. Shi, R. Eberhart, A Modified Particle Swarm Optimizer, *IEEE Proc. Computational Intelligence*, Anchorage, Usa, May 1998.
- [26] J. Kennedy, R. Eberhart, A Discrete Binary Version of the Particle Swarm Algorithm, *Proc. Conf. Systems, Man, And Cybernetics, Piscataway, NJ*, 1997, pp.4104–4108.
- [27] M. E. Baran, F. F. Wu, Network Reconfiguration in Distribution Systems for Loss Reduction and Load Balancing, *IEEE Trans in Power Delivery*, Vol. 4, No. 2,1989, pp. 1401-1407.